Food and Chemical Toxicology 131 (2019) 110531

Contents lists available at ScienceDirect

Food and Chemical Toxicology

journal homepage: www.elsevier.com/locate/foodchemtox

In vitro/in vivo hepatoprotective properties of 1-O-(4-hydroxymethylphenyl)-α-L-rhamnopyranoside from *Moringa oleifera* seeds against carbon tetrachloride-induced hepatic injury

Congyong Sun[1], Wenjing Li[1], Yingkun Liu, Wenwen Deng, Michael Adu-Frimpong, Huiyun Zhang, Qilong Wang, Jiangnan Yu**, Ximing Xu*

Key Lab for Drug Delivery & Tissue Regeneration, Jiangsu Provincial Research Center for Medicinal Function Development of New Food Resources, School of Pharmacy, Jiangsu University, Zhenjiang, 212013, PR China

ARTICLE INFO

Keywords:
Moringa oleifera seeds
1-O-(4-hydroxymethylphenyl)-α-L-rhamnopyranoside
Carbon tetrachloride
Hepatotoxicity
Acute toxicity
Oxidative stress

ABSTRACT

1-O-(4-hydroxymethylphenyl)-α-L-rhamnopyranoside (MPG) is a phenolic glycoside that exists in *Moringa oleifera* seeds with various health benefits, whereas its hepatoprotective effect is lacking clarification. Herein, MPG was isolated from *Moringa oleifera* seeds, and its hepatoprotection against CCl_4-induced hepatotoxicity in L02 cells and ICR mice was investigated. Toxicity studies showed that MPG did not induce significant changes in organ coefficients and histological analysis, as well as exhibited no cytotoxicity. *In vitro* studies indicated that MPG substantially increased cell viability and intracellular SOD activities, and significantly inhibited LDH leakage in CCl_4-treated cells. *In vivo* studies demonstrated that MPG significantly alleviated CCl_4-induced hepatotoxicity in mice, as indicated by diagnostic indicators of hepatic injury, as well as the histopathological analysis. Moreover, MPG reduced the lipid peroxidation levels and regulated the inflammatory cytokines. Notably, MPG substantially suppressed the significant elevation of ROS production in hepatocytes of mice intoxicated with CCl_4. Moreover, TUNEL assay demonstrated that MPG obviously inhibited hepatic apoptosis induced by CCl_4. Altogether, these results suggested that MPG has excellent liver-protecting effects against hepatocytotoxicity induced by CCl_4 in mice and L02 cells, which can be further developed as a valuable functional food additive or drug for the treatment of hepatic injury.

1. Introduction

The metabolism and detoxification of various xenobiotics is the main responsibility of the liver. Nowadays, due to the unhealthy diet and lifestyle, hepatic injuries represent one of the severe and common health concerns in the world. Hepatic injuries are often caused by a number of deleterious agents, such as alcohol, drugs, viral hepatitis, and metabolic disorders, leading to inflammation, necrosis, fibrosis, and cirrhosis. Particularly, acute and chronic liver injuries are mediated significantly by oxidative stress (OS). A common hepatotoxin that is widely used to induce OS associated hepatic injuries in different laboratory animals is carbon tetrachloride (CCl_4), which is applied to assess the protective properties of active ingredients (Jie-Qiong et al., 2014). Principally, CCl_4 accumulates in the parenchyma cells of the liver, while its metabolism is catalyzed by cytochrome P450 (CYP450) to a highly reactive trichloromethyl radical (• CCl_3). This reaction can trigger a cascade of lipid peroxidation process and reactive oxygen species (ROS) overgeneration, which ultimately leads to a toxic state of OS in the liver (Tsai et al., 2010).

In previous studies, traditional herbal treatments of liver injuries were shown to provide some potential drugs (*e.g.* silymarin and glycyrrhizin) which usually act as the scavenger of free radicals, whereas others are anti-oxidant modulators (S. F. Nabavi, Daglia, Moghaddam, Habtemariam and Nabavi, 2014). However, the majority of these

* Corresponding author. Laboratory of Drug Delivery and Tissue Regeneration, Jiangsu Provincial Research Center for Medicinal Function Development of New Food Resources, School of Pharmacy, Jiangsu University, Zhenjiang, 212013, PR China.
** Corresponding author.
E-mail addresses: horizonpacino@sina.cn (C. Sun), 1558293410@qq.com (W. Li), 1347273977@qq.com (Y. Liu), deng4956@yeah.net (W. Deng), adu_frimpongm@yahoo.com (M. Adu-Frimpong), 472998291@qq.com (H. Zhang), wql001wql001@163.com (Q. Wang), yjn@ujs.edu.cn (J. Yu), xmxu@ujs.edu.cn (X. Xu).
[1] These authors contributed equally to this work.

https://doi.org/10.1016/j.fct.2019.05.039
Received 6 May 2019; Received in revised form 22 May 2019; Accepted 24 May 2019
Available online 25 May 2019
0278-6915/

Abbreviations

MOE	*Moringa oleifera* seeds extract
MPG	Moringa phenolic glycoside, 1-O-(4-hydroxymethylphenyl)-α-L-rhamnopyranoside
CCl_4	Carbon tetrachloride
ROS	reactive oxygen species
OS	Oxidative stress
CYP450	cytochrome P 450
BuOH	N-butanol
EtOAc	Ethyl acetate
PE	Petroleum ether
DCM	Dichloromethane; , ddH_2O, deionized distilled water
CMC-Na	Sodium carboxymethylcellulose
TFA	Trifluoroacetic acid
LD50	Lethal dose, 50%
AKP	Alkaline phosphatase
AST	Aspartate aminotransferase
ALT	Alanine aminotransferase
CAT	Catalase
SOD	Superoxide dismutase
GSH-Px	Glutathione peroxidase
T-AOC	Total anti-oxidant capacity
GSH	Reduced glutathione
MDA	Malondialdehyde
MCP-1	monocyte chemoattractant protein-1
IL-1β	interleukin-1β
IL-10	interleukin-10
TNF-a	necrosis factor-alpha
RSD	Relative standard deviation
TUNEL	deoxyribonucleotidyl transferase (TdT)-mediated dUTP-fluorescein isothiocyanate (FITC) nick-end labeling

therapies could hardly stimulate the hepatic function and offer complete protection and regeneration of hepatic cells (S. M. Nabavi, Nabavi et al., 2012). Thus, it is imperative to identify more effective therapies as alternatives for the treatment of liver injuries. The available evidence supports the significance of active ingredients obtained from drug homologous foods for alternative treatment of various disorders, such as anti-cancer (Cheng et al., 2014; Zhou et al., 2017), anti-oxidant (Zhao et al., 2017), anti-diabetes (Gu et al., 2015; Liu et al., 2013a; Zhang et al., 2014), and anti-hyperlipidemia (Liu et al., 2013b). Also, dietary interventions using novel drug homologous food have become attractive for the amelioration of liver dysfunction recently.

Moringa oleifera (also termed 'miracle tree') is part of the *Moringaceae* family, and is widely recognized for its health benefits such as hypoglycemic, anti-cognitive disorder and hypolipidemic (Falowo et al., 2018; Singh et al., 2013). The consumption of the leaves and seeds of *M. oleifera* are usually in the form of vegetables, salad and nutritional supplements, since they contain substantial quantities of amino acids, vitamins, lipids and other phytochemicals (Pinheiro Ferreira, Farias, de Abreu Oliveira and Urano Carvalho, 2008). Recent studies exhibited that the leaves and seeds of *M. oleifera* have anti-inflammation (Rajan et al., 2016), anti-oxidant (Wang et al., 2017), anti-tumor (Sreelatha et al., 2011), immunomodulatory (Anudeep et al., 2016), antibacterial (Neto et al., 2017), hypotensive (Randriamboavonjy et al., 2017), and hypoglycemic (Al-Malki and El Rabey, 2015) activities due to bioactive components such as flavonoids, phenolic glycosides, glucosinolates, lectin, dietary fiber and peptides. However, available data indicate that the i*n vitro* and *in vivo* hepatoprotective effects of a purified phenolic glycoside, 1-O-(4-hydroxymethylphenyl)-α-L-rhamnopyranoside (MPG), has not been studied yet.

In this regard, for the first time, this paper sought to isolate and purify the active compound (MPG) from *M. oleifera* seeds using bioassay-guided fractionation method, and to further investigate its hepatoprotective properties against CCl_4 induced hepatotoxicity, as well as to evaluate the acute toxicity in L02 cells and ICR mice.

2. Materials and methods

2.1. Materials

Absolute ethanol, dichloromethane (DCM), petroleum ether (PE), ethyl acetate (EtOAc), n-butanol (BuOH), castor oil, CCl_4, and dimethylsulfoxide (DMSO) were supplied by Sinopharm Chem. Reagent Co., Ltd. (Shanghai-China). Trifluoroacetic acid (TFA) and sodium carboxymethylcellulose (CMC-Na) were provided by Aladdin Indust. Corp., (Shanghai-China). Methanol and acetonitrile (chromatographically pure) were obtained from TEDIA company, Inc. (Fairfield-USA). The purification of deionized distilled water (ddH_2O) was performed with water purifying system (Millipore Corp., Bedford, MA-USA). Silybin was purchased from Tasly Pharmaceuticals, Inc. (Tianjin-China). Invitrogen (Carlsbad, CA-USA) supplied 3-(4,5-dimethylthiazol-2-yl)-2,5-diphenyltetrazolium bromide (MTT), fetal bovine plasma (FBS), 4',6-diamidino-2-phenylindole (DAPI), RPMI-1640 medium, penicillin-streptomycin and trypsin. The 2,7-Dichlorodihydrofluorescein diacetate (DCFH-DA) for measuring ROS level and the apoptosis detection kit (composed of terminal deoxynucleotidyl transferase-mediated dUTP nick end labeling, TUNEL) were provided by Sigma-Aldrich. Aspartate aminotransferase (AST), alanine aminotransferase (ALT), alkaline phosphatase (AKP), glutathione peroxidase (GSH-Px), malondialdehyde (MDA), reduced glutathione (GSH), superoxide dismutase (SOD), catalase (CAT), lactate dehydrogenase (LDH), total anti-oxidant capacity (T-AOC) and BCA protein commercial reagent kits as well as ELISA test kits, such as monocyte chemotactic protein 1 (MCP-1), interleukin-1β (IL-1β), tumor necrosis factor-alpha (TNF-α) and interleukin-10 (IL-10) were obtained from Nanjing JianCheng Bioengineering. Inst. (Nanjing-China). The other materials were obtained commercially and were of analytical grade.

2.2. Animals

Healthy ICR mice (22 ± 2 g, license number: 201813319, 201813849 and 201814116) were purchased from the Laboratory Animal Research Centre of Jiangsu University (Zhenjiang-China). The housing of the mice was maintained at temperature (20–26 °C), relative humidity (40–70%) and 12 light/12 dark cycle for 3 days with unrestricted access to water and fodder. Fasting in mice lasted for 12 h before the tests with unrestricted water access. The entire animal research protocols for the experiment were performed based on the guidelines issued by the Laboratory Animal Management Committee of Jiangsu University. Each animal was used only once.

2.3. Cell culture

L02 cells (supplied by Cell Bank of Academy of Science, Shanghai-China) were cultured in RPMI-1640 complete medium comprising 10% FBS, nonessential amino acid, penicillin (100 U/mL) and streptomycin (100 μg/mL). The incubation of the cells was conducted in a humidified atmosphere at 37 °C with 5% CO_2.

2.4. Bioassay-guided fractionation and isolation of MPG

2.4.1. Plant materials

Anhui Xiehe Pharmaceutical Co. Ltd., (Anhui-China) provided the *M. oleifera* seeds. The *M. oleifera* seeds were collected in July 2015 from

Yunnan Province, China. It was identified by Prof. Huan Yang from Jiangsu University. A voucher herbarium specimen (SP20151005) was lodged at the School of Pharmacy, Jiangsu University. *M. oleifera* seeds were air-dried at 60 °C overnight, and shattered into powder by pulverizer (XL-20B, Guangzhou XuLang machinery Co., Ltd., Guangzhou, China). The powder was filtered through a 40-mesh sieve and kept at room temperature in a desiccator.

2.4.2. Preparation of crude aqueous extract and bioassay-guided fractionation

Preliminary experiments authenticated that the aqueous extract of *M. oleifera* seeds exhibited significant hepatoprotective activity (data not shown). In view of this, a crude extract was prepared as follows: *M. oleifera* seeds powder (1 kg) was de-oiled twice with PE for 2 h. The dried residual sample was refluxed triply with ddH_2O (liquid to solid ratio, 12) for 3 h at 95 °C. Then, the extracting solutions were mixed, filtered and condensed to 1/10th of the initial volume with a rotary evaporator (Heidolph Co., Germany) under reduced pressure at 60 °C. The concentrate was lyophilized (FreeZone® 6L Freeze Dry Systems, Labconco Corporation, Missouri, USA) to yield the crude aqueous extract (MOE, 181.5 g, extract yield (w/w), 18.1%).

Next, MOE was further fractionated via an organic solvent extraction method to identify the active fractions (Fig. 1A). Sequentially, MOE was dispersed in ddH2O, and triply partitioned with two volumes of DCM, ETOAc and BuOH. The evaporation of the solvent fractions under reduced pressure yielded the respective extracts. The concentrates were dried at 60 °C, weighed and stored at −20 °C until further study. Subsequently, the hepatoprotective activity of the different fractionations were evaluated by the CCl_4-induced hepatotoxicity model to identify the active fractions. Consequently, the bioassay-guided study revealed a significant hepatoprotective activity of MOE-BuOH fraction which was further subjected to compound isolation.

2.4.3. Isolation and quantitative analysis of MPG

As depicted in Fig. 1A, 1-O-(4-hydroxymethylphenyl)-α-L-rhamnopyranoside (MPG) was isolated from the MOE-BuOH fractionation. Briefly, the procedure included two sequential chromatographic steps. Step 1: MOE-BuOH extract was chromatographed via silica gel, eluted with $CHCl_2$–MeOH (20:1–5:1) to afford 5 fractions based on Thin-layer chromatography (TLC) analyses. Then, fraction 3 was again chromatographed over silica gel via gradient elution ($CHCl_2$–MeOH) to achieve homogeneous purification. Step 2: Subfraction 2 was applied to ODS column eluted with MeOH–H_2O (5:95, 10:90, 15:85, and 20:80) to obtain compound MPG. Then, TLC was performed on silica G254 plates (0.2 mm thickness) with the TLC solvent consisting of EtOAc, methanol, formic acid, and water (6:1:1:1). For monitoring analysis, spots were visualized under UV light. Finally, MPG was lyophilized and collected.

MPG ($C_{13}H_{18}O_6$) was unambiguously characterized by ^1H and ^{13}C NMR spectrometry on NMR spectrometer (AVANCE II-400MHz, Bruker Corp., Germany), and the chemical shifts were recorded in DMSO-d_6. Also, UHR-TOF-MS were determined by a mass spectrometer (MAXIS, Bruker Corp., Germany), while the UV spectrum was recorded through HPLC-DAD analysis.

2.5. HPLC-DAD analysis of fractionations and MPG

2.5.1. HPLC-DAD analysis of fractionations

The active fractionation was characterized by RP-HPLC method. Briefly, the analysis of the fractions was performed using an Agilent 1260 liquid chromatography system (Agilent, San Jose-USA) fitted with a G1311B quaternary pump, a G1329B automatic injector, a G1316A thermostatted column compartment, and a G4212B DAD detector.

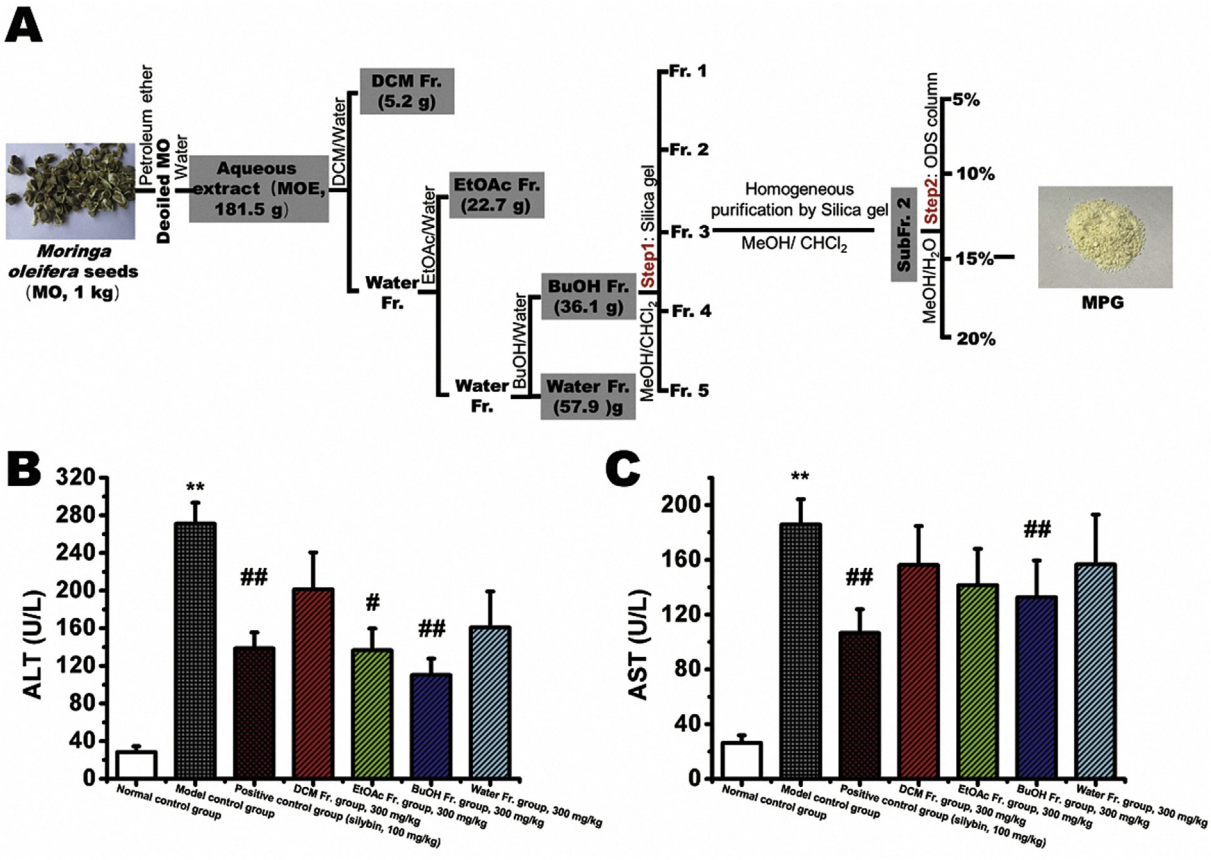

Fig. 1. Scheme for the bioassay-guided fractionations from *Moringa oleifera* seeds (A) and hepatoprotective activity of different fractions on the levels of ALT (B) and AST (C) in CCl_4-induced hepatotoxicity. $^{*}p < 0.05$, $^{**}p < 0.01$, *compared to the normal control group.* $^{\#}p < 0.05$, $^{\#\#}p < 0.01$, *compared to the model control group.*

OpenLAB CDS ChemStation was used to analyze the data. Chromatographic conditions were as follows; separation of the analytes was performed via a Nova-Pak C_{18} column (4.6 × 150 mm, 4 μm, Waters, Milford, MA-USA) with a temperature of 30 °C; the mobile phase was comprised of 0.1% (v/v) TFA aqueous solution (A) and acetonitrile (B) with the gradient elution program: 0–5 min, 5% B; 5.01–40 min, 5–45% B, and post run, 10 min; the flow rate was 1 mL/min and the injection volume was 20 μL. Besides, the detection wavelength was set at 210 nm. Both MOE-BuOH and Subfraction 2 at a concentration of 1 mg/mL were injected into HPLC after filtration through 0.22 μm syringe-driven filter (Jiangsu Mingjie Scientific Instrument Co., Ltd. Nanjing, China).

2.5.2. HPLC-DAD analysis of MPG

The purity of active compound MPG was assessed using HPLC analysis. The mobile phase consisted of 0.1% (v/v) TFA aqueous solution (A) and acetonitrile (B) with isocratic elution of 15% B for separation and 222 nm was the detecting wavelength. An aliquot (20 μL) of MPG (1 mg/mL) was injected into HPLC after filtration through the 0.22 μm syringe-driven filter.

2.5.3. The quantitative analysis of MPG content in the extract

The quantitative analyses of MPG were developed using the above-mentioned chromatographic conditions. Briefly, aliquots (20 μL) of MPG reference solutions (1–50 μg/mL) were injected into HPLC, and the peak areas were measured. Regression analysis was applied to obtain the linear equation based on the plotting of the integral peak area value (y) as ordinate and the reference solution concentration (x, μg/mL) as abscissa. The method validation was conducted in accordance with Chinese Pharmacopoeia 2015. Especially, the validation of specificity, linearity, accuracy, and precision were performed.

2.6. Acute toxicity study

2.6.1. Cytotoxicity in L02 cells

In the development of a novel active compound, acute toxicity investigation is imperative in the pharmacological research. To evaluate the cytotoxicity of MPG in L02 cells, the cell viability was determined with MTT assay method according to our previous study (Huiyun et al., 2019). Briefly, cells at the exponential growth phase were seeded in 96-well plates (1×10^4 cells-per-well, 100 μL) for 24-h incubation. After the cells attained approximately 70–80% confluent, the medium was removed and replaced with a series of concentrations of MPG (from 5 to 100 μg/mL, dissolved in medium with a final solvent concentration of 0.1% DMSO) for 24, 48 and 72 h incubation. After that, MTT (20 μL, 5 mg/mL) was applied to incubate with the cells at 37 °C for 4 h. The MTT medium was removed and formazan crystals were solubilized with DMSO (100 μL) via shaking for 10 min. An automatic microplate reader (BioTek-USA) operating at 570 nm was applied to measure the optical density (OD). Computation of the cell viability was via the equation as follows: Cell viability (%) = $(OD_{sample} - OD_{blank})/(OD_{naive} - OD_{blank}) \times 100\%$, where OD_{sample} was the experimental group optical density; OD_{naive} was the optical density of the control group without treatment and the OD_{blank} was the OD of wells without any sample and seeded cell.

2.6.2. Acute oral toxicity in mice

The oral toxicity of the MPG in ICR mice was further evaluated through the fixed-dose procedure (Li et al., 2012) with the method involving two phases. In the first phase, three groups were formed equally and at random with nine mice. The mice were given MPG via oral gavage at respective doses of 10, 100 and 1000 mg/kg. Then, careful mice observation was carried out for 24 h for toxicity and mortality signs. Based on the first phase findings (no mortality for each group), 50 healthy mice were separated at random into 5 groups (n = 10, male and female ratio was 5:5) for the second phase. All the treatments were administered once through oral gavage. The normal control group received 0.5% CMC-Na, while the MPG-treated groups received doses of 50, 500, 1000 and 2000 mg/kg, accordingly. After a single administration, the entire mice were closely monitored for 4 h and once daily for 14 d in order to evaluate the general behavior, signs of toxicity and mortality. Individual body weights were measured at 0, 7 and 14 d. At the 15th day (after 24 h starvation), all the mice were sacrificed to determine macroscopic alterations of the tissues. Internal organs including heart, liver, lung, kidney, spleen, and brain were collected and weighed before post-fixed in 4% formaldehyde for histological studies. Additionally, organ coefficients were calculated according to the followed equation, Organ coefficient (%) = weight of organ/individual weight of mice × 100%.

2.7. In vitro hepatoprotective activity of MPG

2.7.1. Assessment of cell viability and morphology

To evaluate the *in vitro* hepatoprotective activities of MPG against CCl_4-induced cell death, the cell viability of L02 cells was determined by MTT method (Haihui et al., 2016), and the cell morphology was captured with an inverted optic microscope. Briefly, cells at the exponential growth phase were placed in 96-well plates (2×10^4 cells-per-well, 100 μL) for 24 h incubation. Afterward, varied MPG concentrations (same as section 2.6.1) were used to treat the cells and then CCl_4 (10 mM, diluted with RPMI-1640) was added for 12 h incubation. Then, the morphology of different groups was observed (original magnification 200 ×). Next, MTT (5 mg/mL) was utilized to subsequently incubate the cells at 37 °C for 4 h. At 570 nm, absorbance was recorded to test the cell viabilities, and the results were presented as the percentage of untreated control cells. Silybin (100 μg/mL) was applied as the positive control.

2.7.2. Measurement of ALT, AST, LDH, MDA, and SOD

Additionally, to further assess the hepatoprotective activities of MPG on hepatotoxicity induced by CCl_4, the LDH leakage in medium and the cellular MDA and SOD were measured. Consequently, cells at the exponential growth phase were seeded into 24-well plates (1×10^5 cells-per-well, 500 μL) for 24 h incubation. Later, cells of the naive group were treated with blank medium while negative group treated with CCl_4 (10 mM, diluted with RPMI-1640). In the positive group, the cells were treated with 10 mM CCl_4 and 100 μg/mL silybin, while the cells of the MPG-treated groups were treated with CCl_4 (10 mM) and MPG (at 10, 50 and 100 μg/mL). The cells were cultured for another 24 h, and the media were collected for the evaluation of ALT, AST, and LDH. Subsequently, rubber scrapper was used to detach the cells followed by collection via centrifugation for 10 min at 1500 rpm. The collected cells were sonicated in cold PBS (1 mL) before centrifuging the cell lysates for 30 min at 15000 rpm and 4 °C. Whole homogenates were collected for assay of MDA and SOD.

The activities of ALT and AST, as well as the levels of LDH in the medium were assayed using commercial test kits according to manufacturers' instruction. The content of malondialdehyde (MDA) was determined via thiobarbituric acid (TBA) method (Ohkawa et al., 1979) based on the kit's instructions. The SOD activity in the cells was ascertained with a xanthine-xanthine oxidase method (Joe M. & Irwin, 1969). The MDA content and SOD activity in the cells were normalized to the protein levels.

2.8. In vivo hepatoprotective activity of MPG

2.8.1. Experimental design

On the account of our previous studies (Tong et al., 2011), the CCl_4-induced hepatotoxicity in mice was used to investigate the *in vivo* hepatoprotective properties of MPG. Briefly, the mice were separated at random and equally into 6 groups (n = 10). Subsequently, Group I (normal control group) and Group II (model control group) were given

with CMC-Na solution (0.5%, 20 mL/kg, *i.g.*) daily for 7 consecutive days. Group III (positive control group) was given silybin (100 mg/kg, *i.g.,* dispersed in 0.5% CMC-Na) daily for 7 consecutive days. Simultaneously, the protective effects of different doses of MPG (50, 100 and 150 mg/kg, *i.g.,* suspended in 0.5% CMC-Na) were tested in Groups IV-VI, respectively, for 7 consecutive days. After pretreatment, an acute hepatic injury was inducted on the 8th day. Mice in Groups II-VI were injected with CCl_4 in castor oil (0.2%, 10 mL/kg, *i.p.*) while Group I was given castor oil only.

After 24 h of CCl_4 impairment, all the mice were weighed and sacrificed in a germ-free room. Retro-orbital bleeding was applied to collect the blood samples and then the serum was obtained via centrifugation for 10 min at 3700 rpm. The mice were dissected to expose the liver, prior to hepatic perfusion with a Ca^{2+}-free buffer until the blood was perfused thoroughly. Then, ice-cold phosphate buffer saline (PBS) was used to wash the freshly excised livers prior to weighing and photographing. An amount (0.2 g) of the liver was incubated in 2 mL collagenase at 37 °C for 40 min to separate mice hepatocytes for further flow cytometry analysis. Also, ice-cold PBS (3 mL) was added to liver tissue (0.3 g) and homogenized immediately. For further investigations, the supernatant of the liver homogenate was obtained through centrifugation for 10 min at 3000 rpm. The entire aforesaid processes were carried out at 4 °C, and the samples were kept at −80 °C until subsequent analysis. The remaining liver tissues were post-fixed in 4% formaldehyde for further HE, DAPI, and TUNEL studies.

2.8.2. Biochemical analyses

The serum ALT, AST and AKP activities were selected as the indicators of the hepatic functions and assayed via standard diagnostic kits in terms of the specifications of the manufacturer.

2.8.3. Determination of OS biomarkers

2.8.3.1. Endogenous anti-oxidant enzymes. The SOD, CAT, and GSH-PX were assayed according to the manufacturers' specifications as followed. The SOD activity in liver was measured using a xanthine-xanthine oxidase method. The CAT activity in liver was assessed via Beers and Sizer method (Beers and Sizer, 1952), by determining peroxide decomposition. The GSH-Px activity in liver was measured using the Rotruck method (Rotruck et al., 1973).

2.8.3.2. Non-enzymatic anti-oxidants. The T-AOC and GSH contents were determined according to the manufacturers' instruction. Briefly, the hepatic T-AOC was assayed using ABTS as the substrate. Reduced glutathione (GSH) was determined by the Moron method (Moron et al., 1979) with dithionitrobenzoic (DTNB) as a substrate.

2.8.3.3. Lipid peroxidation level. The MDA content was estimated by TBA method with the standard being 1,1,3,3-tetraethoxypropane. The amount of MDA formed was estimated at 532 nm, and the hepatic MDA content was normalized to the protein levels.

2.9. Assay of ROS level in liver

DCFH-DA, a non-fluorescent substance diffuses passively into cells and esterases can deacetylate DCFH-DA to DCFH. The reaction between ROS and DCFH result in the formation of the fluorescent DCF, which could be determined by fluorescence intensity. Herein, flow cytometry was applied to detect intracellular ROS generation via the fluorescent DCFH-DA probe as stated elsewhere (Peng et al., 2017). In brief, primary mice hepatocytes were isolated via collagenase digestion method as described earlier. Hepatocyte (density of 1×10^6 cells/mL) was re-suspended in PBS (250 μL). Then, the collected hepatocytes were stained at 37 °C for 30 min with 10 μM of DCFH-DA. Flow Cytometry (C6 Plus, Becton, Dickinson and Co., USA) was applied to measure the fluorescence intensity of each cell suspension (300000 cells-per-sample).

2.10. Determination of inflammatory cytokines levels

To determine whether MPG exerts anti-inflammatory activity on injury induced by CCl_4, the levels of the inflammatory cytokines in serum and liver were measured. The liver homogenate was centrifuged (same as stated in section 2.6.1) to collect supernatant for ELISA. Notably, levels of IL-1β, IL-10, MCP-1 and TNF-α in the liver were estimated with ELISA kits concordance with the specification of the manufacturer (results expressed as ng/mg protein). Additionally, IL-1β, MCP-1, IL-10, and TNF-α levels in the serum were also estimated.

2.11. Histopathological study

A qualitative Hematoxylin-Eosin staining (H&E staining) method was performed, for intuitive tissue lesions analysis. In the present study, samples of the removed heart, liver, lung, kidney, spleen, and brain in acute oral toxicity study and livers in hepatoprotective investigations were post-fixed in 4% neutral formaldehyde for 24 h, and further embedded in paraffin for sheet cutting. Then, H&E staining was used to stain sections (4-μm) and observed by upright microscopy (Eclipse Ni–U, Nikon, Japan). Photographs were captured at 100X and 200X magnification, respectively.

2.12. DAPI staining

DNA condensation and nuclear fragmentation in CCl_4-induced hepatotoxicity were investigated by DAPI staining as stated earlier (Caleb Kesse et al., 2016). Concisely, xylene was used to deparaffinize paraffin slices and was rehydrated in varied gradient alcohol (100%, 95%, 90%, 80% and 70%). Afterward, the slices were twice rinsed with PBS, prior to incubation at 37 °C for 10 min with DAPI solution (1 μg/mL), and subsequent rinsing in PBS. The slices were observed with fluorescence microscopy (Nikon, Japan).

2.13. TUNEL assay

TUNEL assay was carried out based on the instruction of the manufacturer. Concisely, the slices were deparaffinized and rehydrated (same as described in section 2.12). Then, the slices were incubated with proteinase K for 20 min. Then the green fluorescein labeled dUTP solution was added before incubating for 1 h at 37 °C. The slices were rinsed with PBS and then photographed via fluorescence microscopy. Subsequently, the samples were stained with the DAB solution. Images were obtained using an upright microscope (Eclipse Ni–U, Nikon, Japan). The TUNEL positive cells showed green fluorescence or brown staining. Ten random visual fields around the centrilobular areas were used to count the TUNEL-positive cells number.

2.14. Statistical analysis

The entire data were presented as mean ± standard deviation (SD). Differences between the distinct groups were statistically evaluated using ANOVA and the Least-Significant Difference (LSD) test. And $p < 0.05$ was considered statistically significant. The entire calculations were performed via statistical software (SPSS version 19.0, SPSS Inc., Chicago, USA). Additionally, all the graphs were drawn using Origin Software® (OriginLab Corp.).

3. Results and discussion

Nature has been a source of biologically active molecules in maintaining human health for millennia, with many useful and significant plant-derived drugs developed (Cragg and Newman, 2013). Specifically, many clinical hepatoprotective drugs (*e.g.* silymarin, kushenin and glycyrrhizin) have been developed from plants. Previous studies demonstrated that a variety of ingredients in *M. oleifera* exert many

health-related benefits. Abundant flavonoids, glucosinolates, and lipids in the leaves, bark and flower of *M. oleifera* are considered to exhibit diverse beneficial bioactivities. Govindarajan et al. (Karthivashan et al., 2015) found that the extract of *M. oleifera* leaves could protect the liver from acetaminophen intoxication possibly through the suppression of CYP 450 isoenzymes, regulation of anti-oxidant enzymes level and modulation of inflammatory cytokines. Likewise, Haddad et al. (El Rabey, Khan, Almutairi and Elbakry, 2017) observed that the low dose of *M. oleifera* seeds powder could ameliorate lipid profile and liver functions in hypercholesterolemic male rats. Besides, Joseph et al. (Randriamboavonjy et al., 2017) posited that the oral administration of *M. oleifera* seeds demonstrated vascular anti-oxidant, anti-inflammatory and endothelial protective effects in spontaneously hypertensive rats. Consequently, these promising evidence of the anti-oxidant activities of *M. oleifera* prompted us to isolate biologically active molecules from *M. oleifera* seeds for the investigation into the hepatoprotective effects of the purified active compound against CCl_4 induced hepatic injury, as well as evaluation of the acute toxicity in L02 cells and ICR mice.

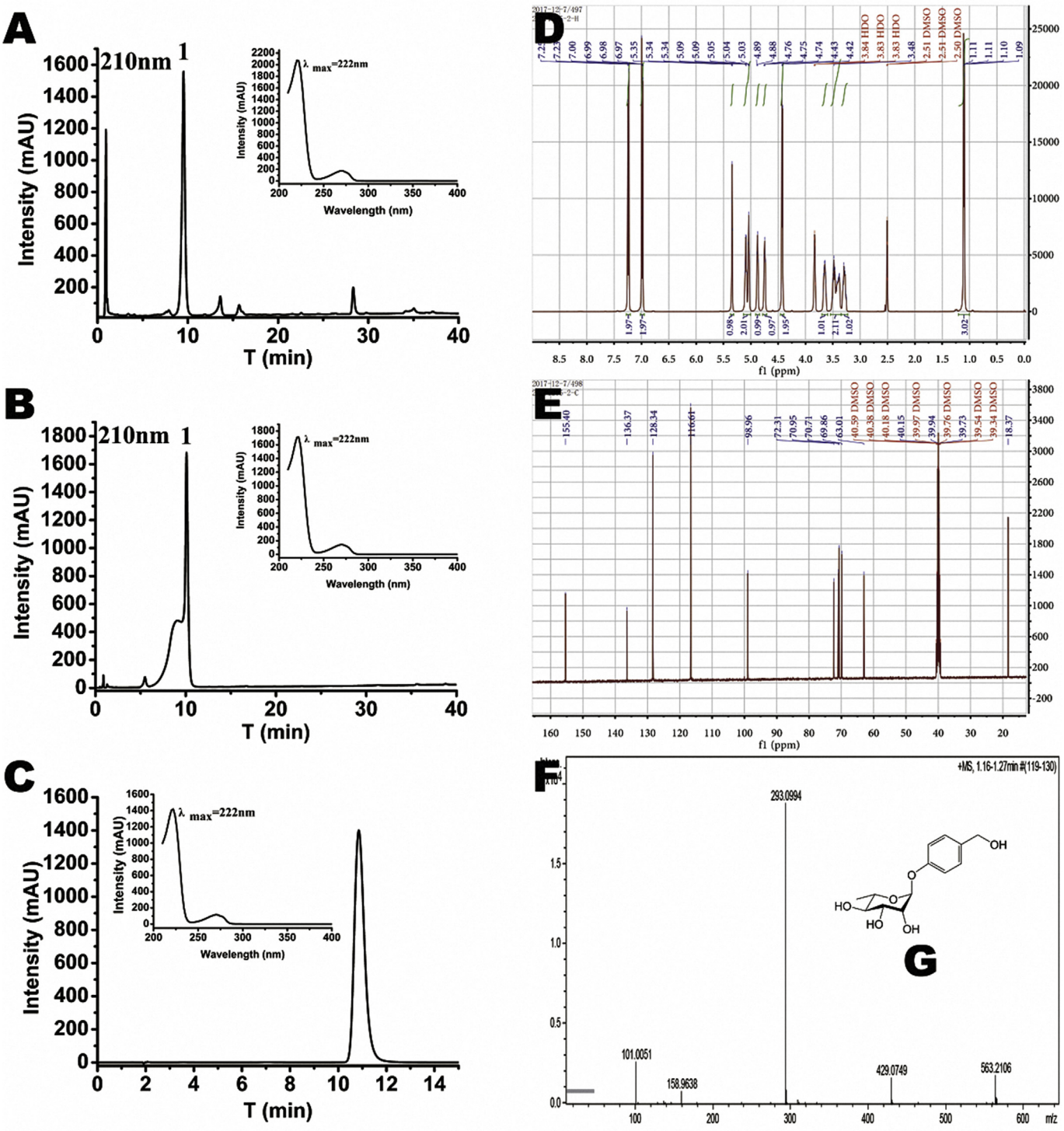

Fig. 2. Purification and identification of MPG. HPLC chromatograms of MOEs-BuOH fractionation (A), Subfraction 2 (B) and purified MPG (C), UV absorption profiles of the major peak were embedded in the HPLC chromatograms; ^{1}H NMR (D) and ^{13}C NMR (E) spectrometry of MPG; UHR-TOF-MS spectrometry of MPG (F); Structure of MPG (G).

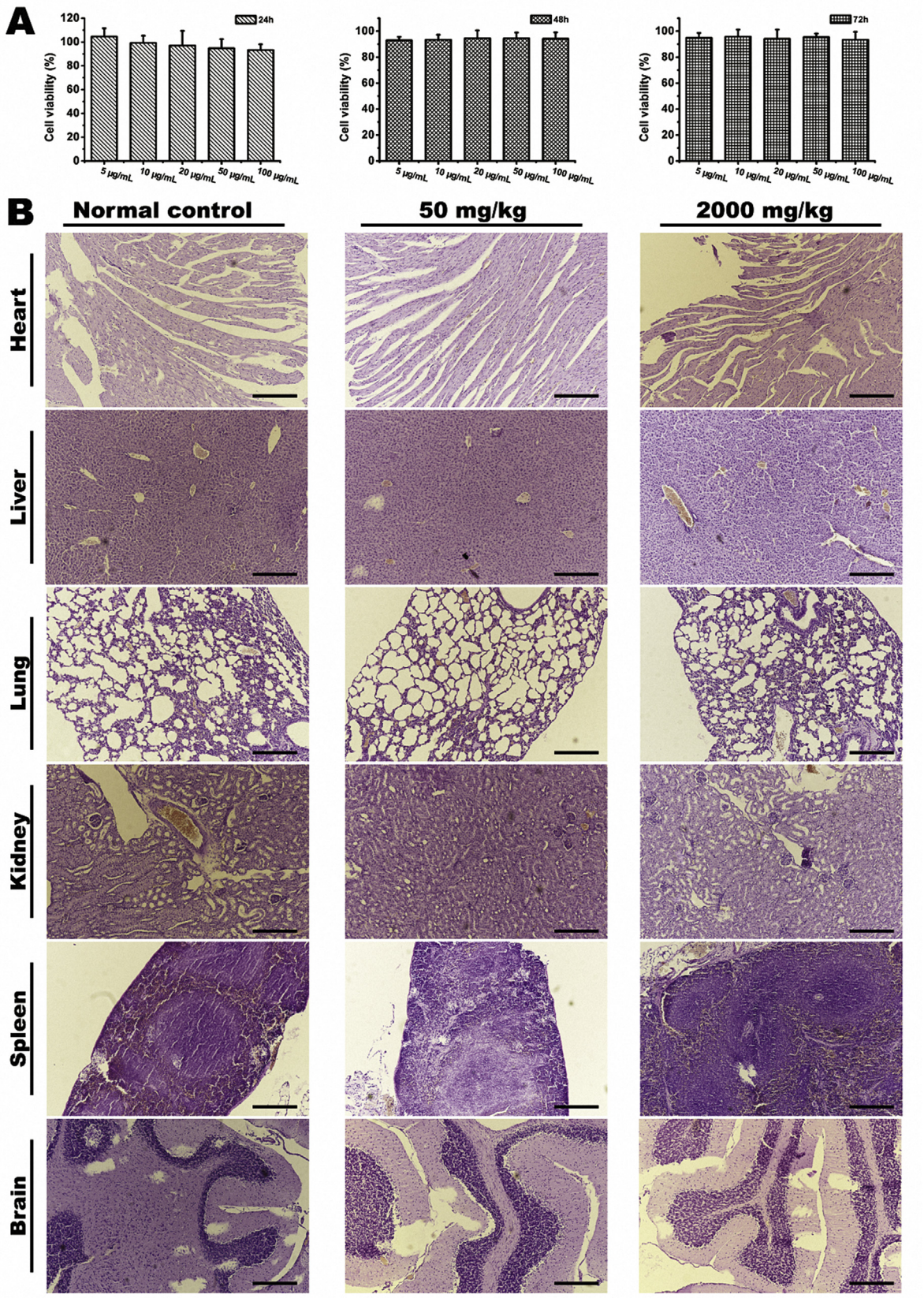

Fig. 3. Acute toxicity of MPG. A: Cytotoxicity of MPG in L02 cells (treated 24, 48 and 72 h); B: Histopathological observations (H&E staining) in the different organs (heart, liver, lung, kidney, spleen and brain) from male mice treated with MPG for 14 days. *Scale bars* 100 μm.

3.1. Bioassay-guided fractionation and HPLC-DAD analysis of MOE-BuOH

Metabolically, liver is a regulatory center for nutrient processing, protein synthesis, energy homeostasis and detoxification. In view of this, liver is mostly vulnerable to chemical-induced injuries. Indeed, CCl_4 is a distinguished toxin in the study of hepatotoxicity induced by xenobiotics. Usually, the oxidative stress and lipid peroxidation caused by CCl_4 metabolism could lead to membrane lipid peroxidation and hepatocellular injury. Normally, under physiological conditions, the enzymes (ALT, AST, and AKP) are confined within the cytoplasm of hepatocyte. However, once hepatic injury occurs, the hepatocellular membrane rupture culminates in the leaking of cellular contents into circulation with consequent increment of these hepatic biomarkers in serum (Drotman and Lawhorn, 1978).

Hence, in this study, CCl_4-induced hepatotoxic injury model was used to screen the hepatoprotective effects of the fractionations and active compound by measuring the serum ALT and AST levels. In mice treated with CCl_4, levels of serum ALT and AST markedly increased comparable to that of the mice in the normal control group (Fig. 1B-C, $^{**}p < 0.01$), indicating the successful establishment of CCl_4-induced hepatotoxicity mice model. After the step-by-step screening of different fractionations, the oral administration of MOE-BuOH at 300 mg/kg was found to demonstrate the maximum hepatoprotective effect, which substantially decreased the serum ALT and AST levels (Fig. 1B-C, $^{\#\#}p < 0.01$). Afterward, the MOE-BuOH fraction was analyzed with the HPLC-DAD. The chromatograms showed that the MOE-BuOH extract had a major compound, giving rise to peak 1 (64.11%, retention time = 9.52 min) as depicted in Fig. 2A. Therefore, the MOE-BuOH fraction was further processed to isolate the main compound, while the chemical structure was accordingly identified.

3.2. Isolation and quantitative analysis of MPG

The MOE-BuOH fraction was further fractionated via two sequential chromatographic steps in order to identify the active compounds. As depicted in Fig. 2B, after homogeneous purification, the content of the target compound in Subfraction 2 was increased. Finally, a white amorphous powder (~2 g) was obtained through ODS column purification. The chromatograms demonstrated that MPG achieved a baseline separation with excellent peak shape (Fig. 2C). The retention time of MPG was 10.85 min. Additionally, λ_{max} of UV spectrum in HPLC analysis were 222 and 272 nm. The purity of MPG was confirmed to be 99.60% based on the area normalization method (Qilong et al., 2018). Additionally, the ^{1}H and ^{13}C NMR spectrometry are shown in Fig. 2D-E. As depicted in Fig. 2F, UHR-TOF-MS m/z 293.0994 was [M + Na], while 563.2106 was [2M + Na] with the determined molecular weight of MPG to be 270 ($C_{13}H_{18}O_6$). Collectively, the compound was unambiguously characterized to be MPG, and its structure (Fig. 3G), was established in accordance with a previous study (Faizi et al., 1995). Purified MPG was stored at −20 °C pending further investigation.

The MPG content was quantified in the MOE-BuOH extract through the development and validation of an efficient HPLC method. The specificity, linearity, accuracy, and precision of the method were evaluated. The standard curve was linearly regressed ($y = 50.011x + 7.5331$, $r^2 = 0.9998$) with the relative-standard deviation values for intra-day precision and inter-day precision ranging from 0.46 to 1.57%. Likewise, spiked samples recovery ranged from 99.87 to 101.16% (Table 1), indicating that the established analytical method was appropriate and accurate. Hence, the established method was suitable for accurately quantifying MPG in the extract. Consequently, the content of MPG in the MOE-BuOH extract was estimated to be 88.9 mg/g of MOE-BuOH extract.

3.3. Acute toxicity study of MPG

For novel active compounds or fractions, toxicity is a significant concern. In the present report, the effect of MPG on cell viability was investigated for the first time. In this regard, the MTT assay was applied to analyze the cell viability of the L02 cells after treatment with MPG (5–100 μg/mL) for 24 h, 48 h, and 72 h. As shown in Fig. 3A, no notable cytotoxic effects were observed in the cell viability at 24 h, 48 h, and 72 h, indicating the low cytotoxicity and high biocompatibility of MPG. Based on this result, the concentrations (viz., 10, 50, and 100 μg/mL) were chosen for subsequent *in vitro* hepatoprotective studies.

On the other hand, MPG was evaluated in terms of mortality in mice. As indicated in Table 2, no animal deaths were observed. No obvious variations were discovered in the mucous membrane or fur, skin and eyes colors. During the 2-week period, the animals showed neither behavioral nor physiological incapacity. The differences in body weight gained in the normal control and the MPG-treated mice during the experimental period are presented in Table 2. In both male and female mice, the body weight of MPG-treated groups increased gradually during the study period, but was statistically not different. Furthermore, in comparison with the control group, the coefficients of organs, viz., heart, lung, spleen, liver, kidney, and brain of the MPG-treated mice indicated no significant changes, except the spleen in MPG-treated (2000 mg/kg) group (Table 2). Spleen weights are deemed to be sensitive indicators of stress, physiologic perturbations and immunotoxicities (immune depletion or stimulation) (Michael et al., 2007). However, spleen weights did not often correlate with histopathologic findings. Thus, histopathology associated with dosage-dependent spleen weight alterations were considered as more sensitive indicators of immunotoxicities (Michael et al., 2007). In this study, dosage-dependent spleen weight changes were not observed. Additionally, histological studies showed no macroscopic tissue injury in both male (Fig. 3B) and female mice (data not shown). Collectively, lethal dose (LD_{50}) of MPG was greater than 2000 mg/kg and did not cause any mortality or obvious organ changes in the mice. According to Fixed-dose procedure, a chemical substance with LD_{50} greater than 2000 mg/kg is considered as practically non-toxic. Hence, MPG could be generally regarded as relatively safe and quite well tolerated.

3.4. In vitro hepatoprotective activity of MPG

3.4.1. MPG increased the cell viability

In order to induce oxidative damage and hepatotoxicity in L02 cells, varied concentrations of CCl_4 were used to treat the cells, while the MTT assay was applied to screen the IC_{50} of CCl_4 concentration. Actually, CCl_4-induced cytotoxicity was concentration dependent (data not shown), and 10 mM was selected to induce hepatotoxicity in the following experiments. As depicted in Fig. 4A, the relative cell viability of L02 cells after CCl_4 exposure decreased to 43.1 ± 4.2%, indicating that CCl_4 caused significant toxicity. However, silybin and MPG exhibited strong hepatoprotective activities by increasing cell viability. Silybin (100 μg/mL), the positive control, protected the cells by causing a significant elevation of cell viability to 55.0 ± 8.8%. Similarly, incubation with MPG (10, 50, 100 and 200 μg/mL) significantly protected the cells. Particularly, the relative cell viability of MPG (100 μg/mL)

Table 1
Intra-day and inter-day precision and accuracy of MPG in QC samples (n = 5, mean ± SD).

Nominal concentration (μg/mL)	Intra-day precision[a]	Inter-day precision[a]	Accuracy[a,b]	
	RSD (%)	RSD (%)	Recovery (%)	RSD (%)
1.5	0.46			
8	0.58	0.76	99.87 ± 1.29	0.69
40	1.57			

[a] Limits: RSD: < 5%.
[b] Spiked samples with MPG standard solution at 4 μg/mL.

Table 2
The observation, changes of body weight gain and organ coefficients of ICR mice after a single administration (*i.g.*) of different dosages of MPG during acute toxicity study (n = 5, mean ± SD).

Group		Death/total and toxic symptom	Weight			Parameter					
Dosage (mg/kg)	Sex		Day 0 (g)	Day 7 (g)	Day 15 (g)	Heart coefficient	Liver coefficient	Spleen coefficient	Lung coefficient	Kidney coefficient	Brain coefficient
Normal control	Male	0/5, None	19.4 ± 1.0	27.4 ± 1.4	30.2 ± 1.5	0.432 ± 0.035	4.343 ± 0.241	0.369 ± 0.028	0.575 ± 0.035	1.115 ± 0.031	1.481 ± 0.038
	Female	0/5, None	19.6 ± 1.8	25.2 ± 1.0	26.0 ± 1.4	0.503 ± 0.026	5.434 ± 0.425	0.377 ± 0.046	0.681 ± 0.071	1.777 ± 0.090	1.690 ± 0.124
50	Male	0/5, None	19.4 ± 1.0	26.8 ± 1.9	30.2 ± 1.6	0.447 ± 0.047	4.666 ± 0.316	0.303 ± 0.053	0.572 ± 0.032	1.166 ± 0.101	1.522 ± 0.037
	Female	0/5, None	19.2 ± 1.2	25.6 ± 1.6	26.8 ± 1.2	0.507 ± 0.033	5.315 ± 0.504	0.335 ± 0.040	0.619 ± 0.066	1.802 ± 0.137	1.659 ± 0.124
500	Male	0/5, None	18.8 ± 1.0	26.4 ± 1.0	30.4 ± 2.1	0.432 ± 0.020	4.560 ± 0.191	0.361 ± 0.053	0.564 ± 0.114	1.130 ± 0.066	1.363 ± 0.116
	Female	0/5, None	19.6 ± 0.5	26.8 ± 0.9	27.2 ± 1.0	0.505 ± 0.021	5.713 ± 0.830	0.324 ± 0.048	0.622 ± 0.037	1.847 ± 0.244	1.572 ± 0.097
1000	Male	0/5, None	19.6 ± 0.5	27.2 ± 1.2	29.6 ± 1.2	0.451 ± 0.057	4.513 ± 0.273	0.310 ± 0.043	0.610 ± 0.083	1.243 ± 0.073	1.568 ± 0.106
	Female	0/5, None	19.4 ± 1.2	25.4 ± 1.4	26.6 ± 1.4	0.499 ± 0.029	4.671 ± 0.295	0.377 ± 0.056	0.611 ± 0.112	1.723 ± 0.173	1.671 ± 0.114
2000	Male	0/5, None	19.0 ± 0.6	26.6 ± 0.8	28.4 ± 1.6	0.409 ± 0.044	4.020 ± 0.220	0.273 ± 0.041*	0.560 ± 0.049	1.096 ± 0.130	1.562 ± 0.108
	Female	0/5, None	19.2 ± 1.5	24.2 ± 1.2	25.0 ± 1.3	0.545 ± 0.040	4.941 ± 0.377	0.354 ± 0.067	0.670 ± 0.053	1.735 ± 0.109	1.811 ± 0.141

reached 70.7 ± 2.3% ($^{###}p < 0.001$). Additionally, in the morphological observation (Fig. 4B), reduced apoptotic bodies in the MPG-treated cells also confirmed the cytoprotective effect of MPG.

3.4.2. MPG prevented the LDH leakage

The MPG protective effect against hepatotoxicity in L02 cells inducted with CCl_4 was also evaluated via measurement of the LDH leakage in the medium. As depicted in Fig. 4C, compared with the untreated cells, substantial LDH level elevation in the supernatant of CCl_4-treated cells was observed ($^{***}p < 0.001$). Contrariwise, incubation with MPG remarkably prevented the leakage of LDH in a dose-dependent manner ($^{#}p < 0.05$, $^{###}p < 0.001$).

3.4.3. MPG reduced oxidative stress

Furthermore, oxidative stress (OS) in CCl_4 treated L02 cells was also evaluated by determining the cellular levels of SOD and MDA. As depicted in Fig. 4D-E, CCl_4 exposure induced severe oxidative stress in the cultured L02 cells culminating in significant elevated levels of MDA ($^{***}p < 0.001$) and diminished SOD activity ($^{***}p < 0.001$). However, these variations were restored by MPG pretreatment. Notably, compared with the CCl_4 model group, co-incubation of MPG with the CCl_4 led to statistically significant decreases in MDA production and obvious increases in cellular SOD levels in a dosage-dependent manner. Likewise, these effects were similar to that of the silybin treated group. These findings affirm the hepatoprotective effects of MPG.

3.5. In vivo hepatoprotective activity of MPG

It has been reported that CCl_4 is mainly metabolized by CYP450 system to the highly reactive radicals (•CCl_3 and CCl_3OO•) (Tsai et al., 2010), culminating in oxidative degradation of lipids in the membrane, hepatocellular injury, centrilobular necrosis, and steatosis. Moreover, free radicals could bind with nucleic acid and protein thus interfering with the synthesis of nucleic acid and protein and eventually culminate in liver cell death (Nada et al., 2010; Recknagel et al., 1989; Valko et al., 2007). Hence, oxidative stress and ensuant lipoperoxidation have been considered principal mechanisms involved in CCl_4-induced hepatotoxic injury. In the *in vivo* study, liver weight, serum markers (ALT, AST, and AKP) and important OS indicators (SOD, CAT, GSH-Px, T-AOC and GSH) in livers, as well as histological studies of CCl_4-induced mice were investigated.

3.5.1. MPG reduced the abnormal enlargement in liver weight

Obvious increased liver weight and representative liver hypertrophy images were observed in mice intoxicated with CCl_4 (Fig. 6D, Table 3, $^{*}p < 0.05$), suggesting that CCl_4 could cause hepatic hypertrophy in mice (Chen et al., 2012). Pretreatment with silybin and MPG substantially reduced the relative liver weight in comparison with the model ($^{#}p < 0.05$, $^{###}p < 0.001$).

3.5.2. MPG decreased the serum ALT, AST, and AKP

Remarkable elevation of serum ALT and AST levels in mice treated with CCl_4 in comparison with the normal control group were observed ($^{***}p < 0.001$). By contrast, ALT and AST levels were markedly decreased in a dosage-dependent manner in silybin and MPG pretreated mice, which indicate liver recovery towards normalcy (Table 3, $^{#}p < 0.05$, $^{##}p < 0.01$, $^{###}p < 0.001$). Particularly, ALT levels in 150 mg/kg and AST levels in three dosages of MPG treatment groups were comparable with those of the silybin treatment group. Additionally, AKP, another enzyme marker for the plasma membrane and endoplasmic reticulum (Kwo et al., 2017) was also used to evaluate the hepatoprotective effect. As showed in Table 3, serum AKP levels were markedly increased in the CCl_4-treated mice while that of the MPG treatment groups decreased in a dosage-dependent manner compared with the model group ($^{##}p < 0.01$, $^{###}p < 0.001$). The aforementioned results suggested that MPG has hepatoprotective effects against

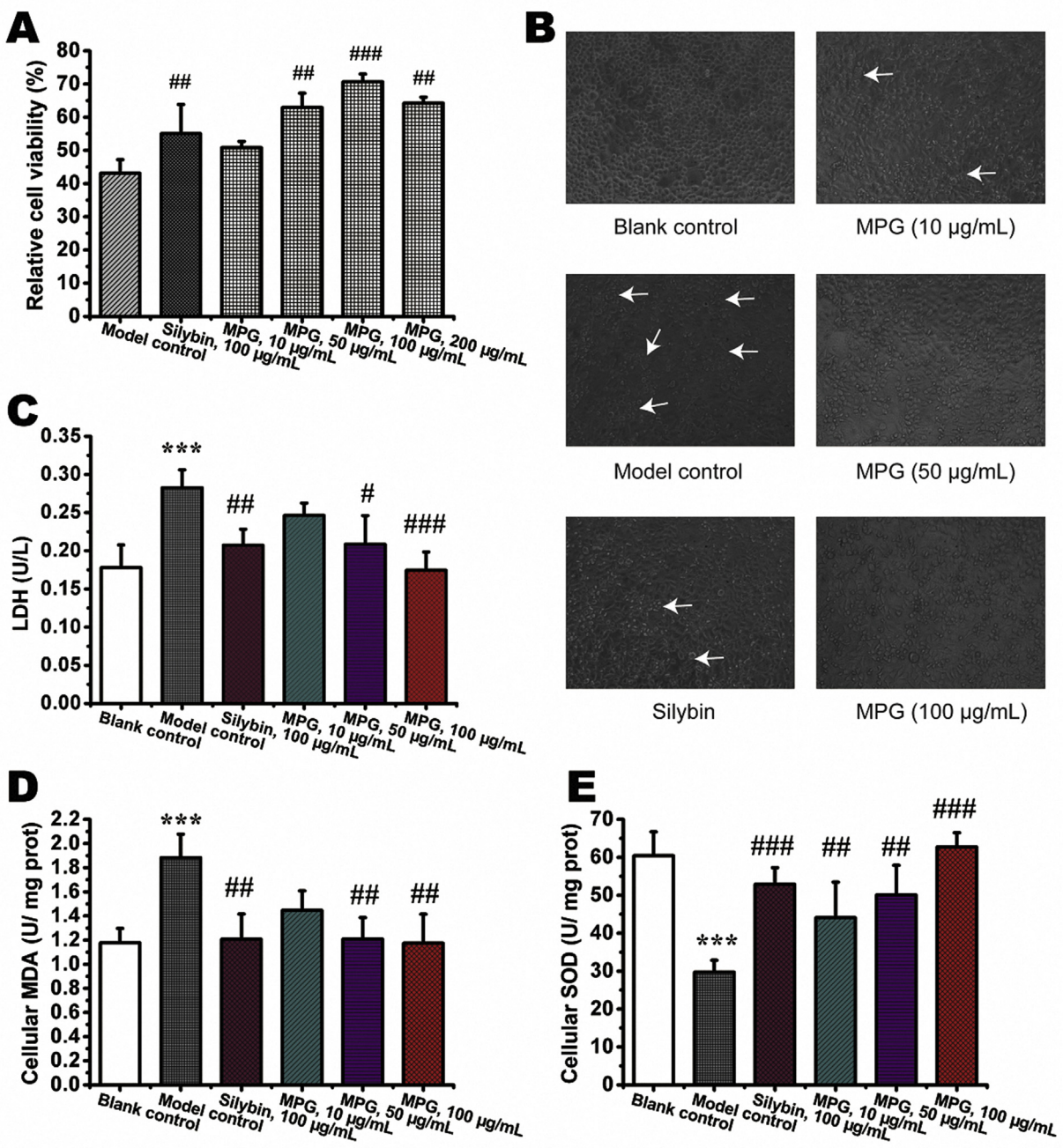

Fig. 4. *In vitro* hepatoprotective activity of MPG. Effect of MPG on the relative cell viability (A) and morphological changes (B) in CCl_4-treated L02 cells; Effect of MPG on LDH leakage (C), MDA levels (D) and SOD activities (E) in CCl_4-treated L02 cells. L02 cells were incubated with CCl_4 (10 mM) and various concentrations (10, 50 and 100 μg/mL) of MPG for 12 h. The morphology of different groups was observed. The white arrows represent the apoptotic bodies. MTT assay was performed to measure the relative cell viability. The LDH leakage in the medium and the cellular MDA and SOD were measured. $^{***}p < 0.001$, *compared to the normal control group.* $^{##}p < 0.01$, $^{###}p < 0.001$, *compared to the model control group.*

hepatotoxicity in mice intoxicated with CCl_4.

3.5.3. MPG suppressed OS induced by CCl_4

Mechanistically, when the ROS generation overwhelms the anti-oxidant capacity, injury to cellular biopolymer (hepatotoxicity) may result (Brenner et al., 2013). For example, the CCl_4-induced oxidative damage could trigger a cascade of chemical processes that perturb cellular functions, increase lipoperoxidation and endogenously alter the levels of the enzymatic and nonenzymatic anti-oxidant systems. Hence, the antioxidation and suppression of free radical production are crucial with respect to liver protection.

On one hand, the integral protective mechanism is the processes that cells utilize the principal antioxidative enzymes (SOD, CAT, and GSH-PX) endogenously to prevent OS. Usually, these enzymes are regarded as first-line of defense system to scavenge ROS in an organism, thereby keeping the status of redox equilibrium (Srinivasan, 2014). Pertinently, GSH-Px and SOD could metabolize hydroperoxide to non-toxic compounds and culminate in the termination of lipoperoxidation chain reaction via lipohydroperoxide removal from cellular membrane. Likewise, CAT could catalyze the decomposition of H_2O_2 into O_2 to prevent cell injury. These enzymes can expeditiously countervail the OS under physiologic conditions. Contrariwise, exposure to CCl_4 could decrease SOD and CAT activities and break down the GSH-dependent anti-oxidant defense system. As displayed in Fig. 5A-C, the activities of

Table 3
Hepatoprotective activity of MPG on liver weight and levels of ALT, AST and AKP in CCl_4-induced hepatotoxicity (n = 10, mean ± SD).

Serial no.	Groups	Liver weight (g)	ALT (U/L)	AST (U/L)	AKP (U/L)
I	Normal control	0.78 ± 0.07	19.90 ± 3.90	27.14 ± 2.14	22.04 ± 6.29
II	Model control	0.96 ± 0.08*	212.97 ± 13.18***	148.36 ± 21.91***	35.46 ± 7.33*
III	Silybin 100 mg/kg)	0.80 ± 0.14$^{\#}$	150.46 ± 15.67$^{\#\#}$	88.39 ± 12.64$^{\#\#\#}$	24.20 ± 5.08$^{\#\#}$
IV	MPG 50 mg/kg)	0.88 ± 0.15	178.36 ± 36.82	87.24 ± 12.97$^{\#\#\#}$	23.99 ± 8.74$^{\#\#}$
V	MPG 100 mg/kg)	0.79 ± 0.14$^{\#}$	173.04 ± 23.73$^{\#}$	75.03 ± 12.96$^{\#\#\#}$	22.35 ± 4.42$^{\#\#}$
VI	MPG 150 mg/kg)	0.72 ± 0.09$^{\#\#\#}$	153.00 ± 16.14$^{\#\#}$	59.49 ± 18.41$^{\#\#\#}$	19.42 ± 7.84$^{\#\#\#}$

$^{*}p < 0.05$, $^{***}p < 0.001$, compared to the normal control group.
$^{\#}p < 0.05$, $^{\#\#}p < 0.01$, $^{\#\#\#}p < 0.001$, compared to the model control group.

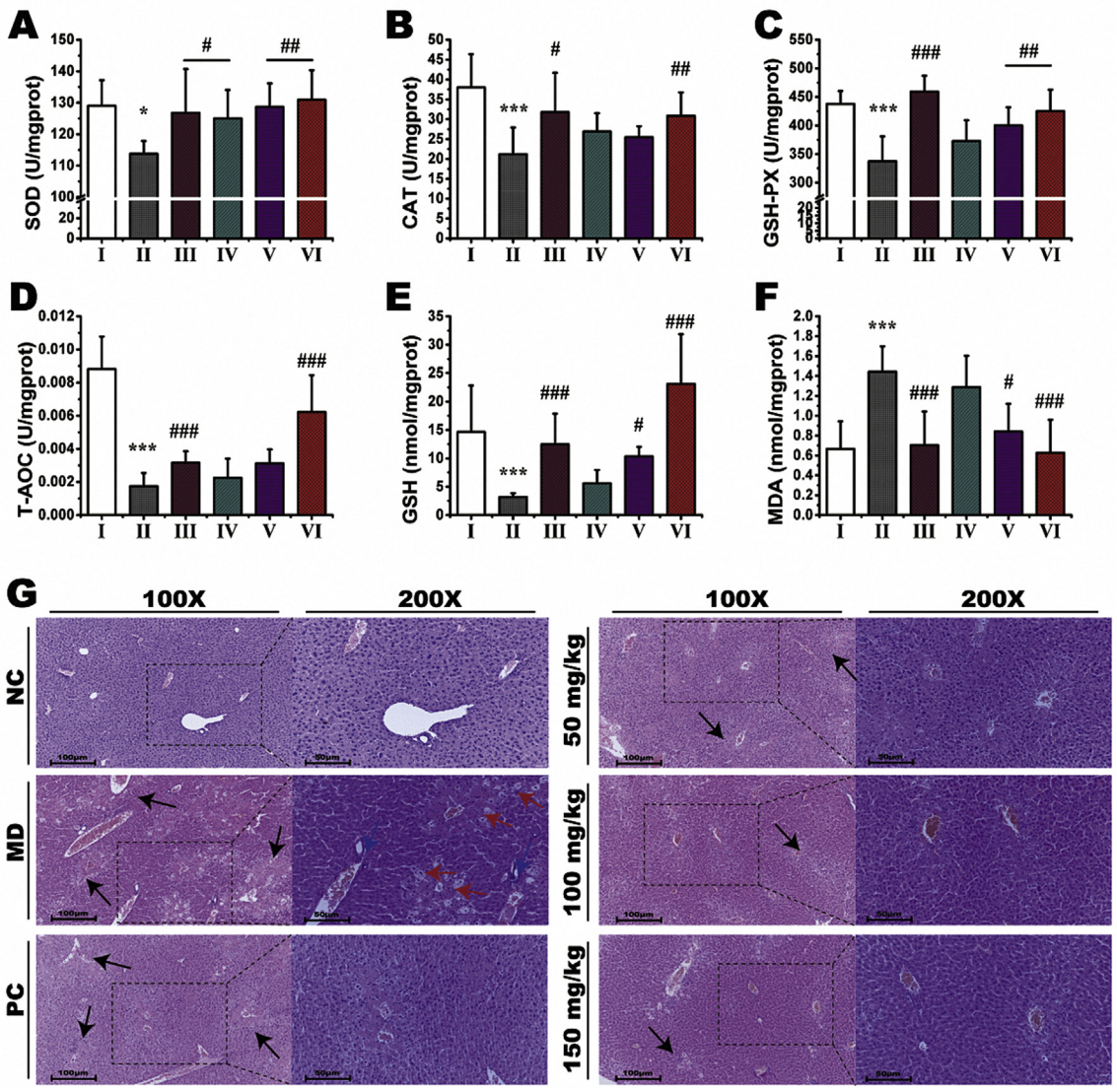

Fig. 5. Hepatoprotective activity of MPG against CCl_4-induced hepatotoxicity in mice. A–F: Effects of MPG on hepatic endogenous enzymatic anti-oxidant activities (SOD, CAT, and GSH-Px), non-enzymatic anti-oxidant activities (T-AOC and GSH) and hepatic MDA level; G: Protective properties of MPG against CCl_4-induced histopathological alterations (H&E staining). NC (I) and MD (II) groups (0.5% CMC-Na solution, 20 mL/kg, *i.g.*), PC (III, silybin, 100 mg/kg, *i.g.*) and MPG-treated groups (VI: 50 mg/kg, V: 100 mg/kg, VI: 150 mg/kg, *i.g.*) were treated for 7 consecutive days. After pretreatment, an acute liver injury was experimentally induced by CCl_4 (0.2% in castor oil, 10 mL/kg, *i.p.*). Biochemical indicators, inflammatory cytokines, and histopathological studies were investigated. *$^{*}p < 0.05$, $^{**}p < 0.01$, $^{***}p < 0.001$, compared to the normal control group. $^{\#}p < 0.05$, $^{\#\#}p < 0.01$, $^{\#\#\#}p < 0.001$, compared to the model control group. Black arrows: centrilobular necrosis and loss of cellular boundaries with disruption of membranes. Red arrows: vacuolation and cell swelling. Blue arrows: inflammation. Scale bars 50 and* 100 μm. (For interpretation of the references to color in this figure legend, the reader is referred to the Web version of this article.)

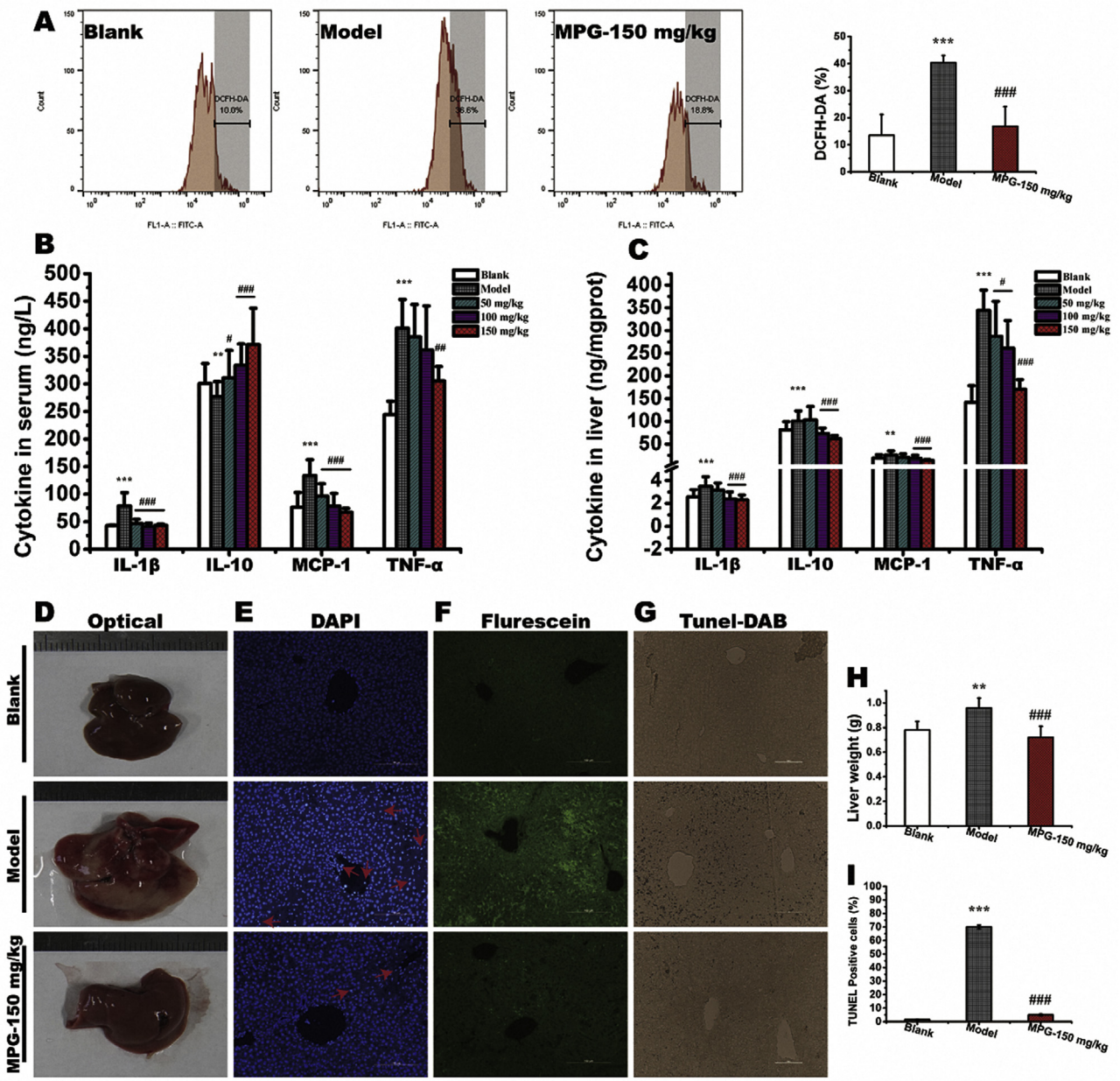

Fig. 6. MPG inhibited CCl_4-induced ROS production and apoptosis, as well as regulated inflammatory cytokines in mice. Effects of MPG on ROS generation and statistical analysis of DCFH-DA percentage in isolated mice hepatocytes (A); Effects of MPG on CCl_4-induced hepatic inflammatory cytokines in serum (B) and liver (C); Representative optical images of mice livers after CCl_4-induced hepatotoxicity (D); Typical micrographs of DAPI stained nuclei (E), TUNEL fluorescent positive cells (F) and DAB stained cells (G) in blank, model and MPG-treated groups. Statistical analysis of liver weight (H) and TUNEL fluorescent images (I). After pretreatment of MPG (150 mg/kg), an acute liver injury was experimentally induced by CCl_4 (0.2% in castor oil, 10 mL/kg, *i.p.*). Mice hepatocytes were separated for flow cytometry analysis and fresh livers were collocated and fixed for the DAPI and TUNEL staining. $^{**}p < 0.01$, $^{***}p < 0.001$, *compared to the normal control group.* $^{\#\#\#}p < 0.001$, *compared to the model control group. Red arrows: condensed or damaged nuclei. Scale bars* 100 μm. (For interpretation of the references to color in this figure legend, the reader is referred to the Web version of this article.)

CAT, SOD and GSH-Px substantially diminished in the liver of CCl_4-treated mice than the normal counterpart ($^{*}p < 0.05$, $^{***}p < 0.001$). However, MPG pretreatment dose-dependently increased the activities of SOD, CAT and GSH-Px in liver ($^{\#}p < 0.05$, $^{\#\#}p < 0.01$). Notably, the SOD, GSH-Px and CAT activities in 150 mg/kg of MPG treatment group were elevated substantially, which even reached the same level as that of the silybin treatment group, indicating that the activities of these anti-oxidants may be restored and maintained by MPG.

Besides, T-AOC reflects the capability of the non-enzymatic anti-oxidant system in defending the body against ROS, while GSH (also non-enzymatic anti-oxidant) is the first line of defense. Under normal physiological conditions, GSH mostly exists in the reduced form. Usually, GSH-Px detoxifies peroxides during injuries by reacting with GSH. Consequently, OS caused decreased GSH content in the liver. As portrayed in Fig. 5D-E, the T-AOC and GSH levels of model mice were markedly decreased comparable to the control group ($^{***}p < 0.001$). Pretreatment of MPG greatly elevated the T-AOC and GSH levels in the liver ($^{\#}p < 0.05$, $^{\#\#\#}p < 0.001$). More importantly, T-AOC and GSH levels in mice supplemented with 150 mg/kg of MPG were higher than those in mice pretreated with silybin, pointing obvious strengthening of the non-enzymatic anti-oxidant system.

3.5.4. MPG decreased the hepatic lipid peroxidation levels

In addition, the overproduction of reactive substances culminates in

a free radical-mediated lipoperoxidation, which involves cascade reactions of free radicals with unsaturated lipids, leading to the production of hydroperoxide and metabolism of lipids to low molecular weight fragments. Pertinently, the hepatic formation of MDA is regarded as one of the indicators of oxidative stress causing hepatic injuries (Ganesan et al., 2018). As depicted in Fig. 5F, the MDA contents in the model cohort raised substantially than the control group ($^{***}p < 0.001$), indicating severe hepatic OS. However, the pretreatment of MPG substantially decreased the liver MDA level. Notably, the MDA levels were markedly reduced at 150 mg/kg of MPG ($^{\#\#\#}p < 0.001$) which was equivalent to the silybin and normal control groups. These results revealed that the antihepatotoxic effect of MPG perhaps is related closely with lipid OS relief.

3.5.5. MPG ameliorated histopathology status of CCl_4-injured liver

The findings of histopathology confirmed the hepatoprotective activity of MPG. Representative sections of the liver from each group are presented in Fig. 5G. In normal livers, the sections exhibited distinct hepatic cells with cytoplasm that is well-preserved as well as spectacular nuclei, normal sinusoids and epithelium lining, and no visible lesion in the central veins. In the model control group, CCl_4-induced liver damage revealed large necrotic areas with a total loss of liver architecture, such as loss of cellular boundaries, condensed nuclei, cell swelling, centrilobular necrosis and massive inflammation. Additionally, sinusoidal congestion, central vein crowding and apoptosis, intense destruction in the lobular structure and severe fibrosis were also evident. In the positive control group, mice treated with silybin demonstrated no obvious necrosis coupled with nearly normal hepatic architectural integrity as compared with the model control group. In MPG groups, mice treated with MPG (50, 100 and 150 mg/kg) demonstrated gradual restoration of liver architecture to normalcy. The central venules were visible with improved sinusoids, while only very slight lymphocyte infiltrations were observed. MPG-treated livers exhibited little degenerative cells, less necrosis, and hepatocyte regeneration, which suggest restoration to the normal hepatic structure. In particular, high dose of MPG treatment showed a superior effect on improving liver tissues than the positive control silybin. Evidently, the histological observations of liver complementally proved that MPG treatment prevented cytoplasmic alterations.

3.6. MPG ameliorated ROS level

It is evident that the accumulation of cellular ROS results from elevated ROS generation and/or reduced ROS scavenging capacity (Johnston and Kroening, 1998). In view of the deleterious effect of excessive cellular ROS levels on the biomolecules (DNA, RNA, lipids, and proteins), direct attenuation of ROS levels and oxidative cascade reaction should be presented in the processes of attenuating CCl_4 hepatotoxicity. Based on this assertion, the accumulation levels of ROS in hepatocytes were evaluated in this report via flow cytometry. As indicated in Fig. 6A, compared with the normal group, CCl_4 significantly enhanced levels of intracellular ROS ($^{***}p < 0.001$). However, MPG (150 mg/kg) remarkably attenuated the increased ROS levels, suggesting the involvement of the ROS-mediated pathway in the hepatoprotective effect of MPG. These results indicated that the reduced ROS production could reduce the physiological deterioration and enhance the resistance of liver against CCl_4.

3.7. MPG regulated inflammatory cytokines

In addition to the OS in the CCl_4-induced hepatotoxic injury, the metabolites of CCl_4 do not only cause direct hepatic injury, but also activate inflammatory response, via initiation of Kupffer cells or T-lymphocytes to release pro-inflammatory cytokines (like TNF-α and IL-1β). Also, the stimulation of MCP-1 generation during inflammation culminates in parenchymal cell injury (Torres et al., 2016).

Besides, as a crucial mediator in inflammatory responses, the TNF-α controls the inflammatory network signaling. Thus, TNF-α overgeneration ultimately leads to the development of liver failure (In-Chul et al., 2014). IL-1β is another key factor in immune cells-mediated inflammation in the liver. In this regard, the hepatic IL-1β level is reported to increase in liver injury (Shih-Yi et al., 2017). Corroboratory, our results confirmed that (Fig. 6B-C) in comparison with the untreated mice, CCl_4 treatment caused marked elevations of TNF-α in both serum and hepatic tissue, which is related to increased IL-1β and MCP-1 levels. However, MPG treatment considerably and dose-dependently reduced these pro-inflammatory cytokines ($^{\#}p < 0.05$, $^{\#\#\#}p < 0.001$).

On the other hand, as a prominent cytokine with anti-inflammatory activity, IL-10 suppresses strongly the generation of proinflammatory mediators (Fiorentino, Zlotnik, Mosmann, Howard and O'Garra, 2016). As presented in Fig. 6B-C, after CCl_4 treatment, IL-10 level was raised in the liver but decreased in serum. However, MPG treatments reversed the CCl_4-induced dysregulation of IL-10 levels in both the serum and liver. Consequently, MPG treatments led to a decrease in TNF-α, IL-1β and MCP-1 levels in the liver, as well as elevated IL-10 release in the systemic circulation, which are significant for attenuating CCl_4-inducted inflammation and destruction.

3.8. MPG inhibited the hepatic apoptosis

Apoptosis pathway is partly involved in CCl_4-induced hepatotoxicity. Hence, to further assess the anti-apoptosis effects of MPG in CCl_4-induced apoptosis, we evaluated the DAPI staining and TUNEL assay. Again, DNA condensation and nuclear fragmentation were detected with DAPI. As displayed in Fig. 6E, in the normal control group, the hepatic nuclei were spherical and no visible morphological impairment was observed, however, the nuclei were condensed or even lost in the CCl_4-treated group. On the contrary, pretreatment with MPG (150 mg/kg) attenuated CCl_4-inducted DNA impairment, which was maintained the hepatocellular architecture and function. Additionally, as shown in Fig. 6F-G, few apoptotic hepatic cells were observed in the normal control group, while TUNEL-positive cells in the CCl_4-treated group were increased substantially ($^{***}p < 0.001$). Nonetheless, the positive cells in the group treated with MPG were markedly decreased ($^{\#\#\#}p < 0.001$). Moreover, excessive hepatocyte apoptosis was associated with TNF-α overexpression (Sanches et al., 2014), which is indicated by the aforementioned ELISA assessment, merely the increment was alleviated in the MPG-treated groups.

4. Conclusion

In summary, 1-O-(4-hydroxymethylphenyl)-α-L-rhamnopyranoside (MPG) was purified from *M. oleifera* seeds extracts. Acute oral toxicity results demonstrated the good safety and high biocompatibility of MPG. *In vitro* and *in vivo* antihepatotoxicity studies in the L02 cells and ICR mice manifested that MPG substantially protected the liver against acute hepatotoxicity induced by CCl_4 via anti-oxidant system enhancement, amelioration of the oxidative stress, regulation of inflammatory mediators and anti-apoptosis. These findings indicated that MPG could be developed as a potential hepatoprotective drug, and its application in preventing hepatotoxicity deserves further investigation. Additionally, further detailed studies are on-going to explore the molecular mechanisms involved.

Conflicts of interest

We declare that we have no conflicts of interest to disclose.

Declaration of interests

The authors declare that they have no known competing financial interests or personal relationships that could have appeared to

influence the work reported in this paper.

Acknowledgements

This work was supported by the National Natural Science Foundation of China (Grant 81720108030 and 81773695), National "Twelfth Five-Year" Plan for Science & Technology Support (Grant 2013BAD16B07-1), China Postdoctoral Science Foundation (2017M621658 and 2017M621659), Program for Scientific Research Innovation Team in Colleges and Universities of Jiangsu Province (SJK-2015-4), a project funded by the Priority Academic Program Development of Jiangsu Higher Education Institutions, and the financial support by Key Lab for Drug Delivery & Tissue Regeneration, Jiangsu Provincial Research Center for Medicinal Function Development of New Food Resources. The authors also thank the University Ethics Committee for the kind guidance in the animal experiments.

References

Al-Malki, A.L., El Rabey, H.A., 2015. The antidiabetic effect of low doses of moringa oleifera lam. Seeds on streptozotocin induced diabetes and diabetic nephropathy in male rats. BioMed Res. Int. https://doi.org/10.1155/2015/381040.

Anudeep, S., Prasanna, V.K., Adya, S.M., Radha, C., 2016. Characterization of soluble dietary fiber from Moringa oleifera seeds and its immunomodulatory effects. Int. J. Biol. Macromol. 91, 656–662. https://doi.org/10.1016/j.ijbiomac.2016.06.013.

Beers, R.F., Sizer, I.W., 1952. A spectrophotometric method for measuring the breakdown of hydrogen peroxide by catalase. J. Biol. Chem. 195, 7.

Brenner, C., Galluzzi, L., Kepp, O., Kroemer, G., 2013. Decoding cell death signals in liver inflammation. J. Hepatol. 59 (3), 583–594. https://doi.org/10.1016/j.jhep.2013.03.033.

Caleb Kesse, F., Zhang, H., Wang, Y., Chen, J., Cao, X., Deng, W., ... Xu, X., 2016. Segetoside I, a plant-derived bisdesmosidic saponin, induces apoptosis in human hepatoma cells in vitro and inhibits tumor growth in vivo. Pharmacol. Res. 110, 101–110. https://doi.org/10.1016/j.phrs.2016.04.032.

Chen, J., Mao, D., Yong, Y., Li, J., Wei, H., Lu, L., 2012. Hepatoprotective and hypolipidemic effects of water-soluble polysaccharidic extract of Pleurotus eryngii. Food Chem. 130 (3), 687–694. https://doi.org/10.1016/j.foodchem.2011.07.110.

Cheng, X., Gu, J., Zhang, M., Yuan, J., Zhao, B., Jiang, J., Jia, X., 2014. Astragaloside IV inhibits migration and invasion in human lung cancer A549 cells via regulating PKC-alpha-ERK1/2-NF-kappa B pathway. Int. Immunopharmacol. 23 (1), 304–313. https://doi.org/10.1016/j.intimp.2014.08.027.

Cragg, G.M., Newman, D.J., 2013. Natural products: a continuing source of novel drug leads. Biochim. Biophys. Acta Gen. Subj. 1830 (6), 3670–3695. https://doi.org/10.1016/j.bbagen.2013.02.008.

Drotman, R.B., Lawhorn, G.T., 1978. Serum enzymes as indicators of chemically induced liver damage. Drug Chem. Toxicol. 1 (2), 163–171. https://doi.org/10.3109/01480547809034433.

El Rabey, H.A., Khan, J.A., Almutairi, F.M., Elbakry, M.A., 2017. The low dose of drumsticks (Moringa oleifera L.) seed powder ameliorates blood cholesterol in hypercholesterolemic male rat. Indian J. Biochem. Biophys. 54 (6), 306–313 Retrieved from < Go to ISI > ://WOS:000424315600007.

Faizi, S., Siddiqui, B.S., Saleem, R., Siddiqui, S., Aftab, K., Gilani, A.U.H., 1995. Fully acetylated carbamate and hypotensive thiocarbamate glycosides from Moringa-Oleifera. Phytochemistry 38 (4), 957–963. https://doi.org/10.1016/0031-9422(94)00729-d.

Falowo, A.B., Mukumbo, F.E., Idamokoro, E.M., Lorenzo, J.M., Afolayan, A.J., Muchenje, V., 2018. Multi-functional application of Moringa oleifera Lam. in nutrition and animal food products: a review. Food Res. Int. 106, 317–334. https://doi.org/10.1016/j.foodres.2017.12.079.

Fiorentino, D.F., Zlotnik, A., Mosmann, T.R., Howard, M., O'Garra, A., 2016. IL-10 inhibits cytokine production by activated macrophages. J. Immunol. 197 (5), 1539–1546 Retrieved from < Go to ISI > ://WOS:000385002300003.

Ganesan, K., Jayachandran, M., Xu, B.J., 2018. A critical review on hepatoprotective effects of bioactive food components. Crit. Rev. Food Sci. Nutr. 58 (7), 1165–1229. https://doi.org/10.1080/10408398.2016.1244154.

Gu, J.-f., Zheng, Z.-y., Yuan, J.-r., Zhao, B.-j., Wang, C.-f., Zhang, L., ... Jia, X.-b., 2015. Comparison on hypoglycemic and anti-oxidant activities of the fresh and dried Portulaca oleracea L. in insulin-resistant HepG2 cells and streptozotocin-induced C57BL/6J diabetic mice. J. Ethnopharmacol. 161, 214–223. https://doi.org/10.1016/j.jep.2014.12.002.

Haihui, Z., Xiaoping, L., Jiajia, K., Yuqing, D., Yuanqing, H., Di, Z., ... Xiaobo, S., 2016. Procyanidins, from Castanea mollissima Bl. shell, induces autophagy following apoptosis associated with PI3K/AKT/mTOR inhibition in HepG2 cells. Biomed. Pharmacother. 81, 15–24. https://doi.org/10.1016/j.biopha.2016.04.002.

Huiyun, Z., Congyong, S., Adu-Frimpong, M., Jiangnan, Y., Ximing, X., 2019. Glutathione-sensitive PEGylated curcumin prodrug nanomicelles: preparation, characterization, cellular uptake and bioavailability evaluation. Int. J. Pharm. 555, 270–279. https://doi.org/10.1016/j.ijpharm.2018.11.049.

In-Chul, L., Sung-Hwan, K., Hyung-Seon, B., Changjong, M., Seong-Soo, K., Sung-Ho, K., ... Jong-Choon, K., 2014. The involvement of Nrf2 in the protective effects of diallyl disulfide on carbon tetrachloride-induced hepatic oxidative damage and inflammatory response in rats. Food Chem. Toxicol. 63, 174–185. https://doi.org/10.1016/j.fct.2013.11.006.

Jie-Qiong, M., Ding, J., Zhang, L., Liu, C.-M., 2014. Hepatoprotective properties of sesamin against CCl4 induced oxidative stress-mediated apoptosis in mice via JNK pathway. Food Chem. Toxicol. 64, 41–48. https://doi.org/10.1016/j.fct.2013.11.017.

Joe, M.,M., Irwin, F., 1969. Superoxide dismutase. J. Biol. Chem. 244, 6049–6055. Retrieved from. https://ci.nii.ac.jp/naid/10025613765/en/.

Johnston, D.E., Kroening, C., 1998. Mechanism of early carbon tetrachloride toxicity in cultured rat hepatocytes. Pharmacol. Toxicol. 83 (6), 231–239. https://doi.org/10.1111/j.1600-0773.1998.tb01475.x.

Karthivashan, G., Arulselvan, P., Tan, S.W., Fakurazi, S., 2015. The molecular mechanism underlying the hepatoprotective potential of Moringa oleifera leaves extract against acetaminophen induced hepatotoxicity in mice. J. Funct. Food. 17, 115–126. https://doi.org/10.1016/j.jff.2015.05.007.

Kwo, P.Y., Cohen, S.M., Lim, J.K., 2017. ACG clinical guideline: evaluation of abnormal liver chemistries. Am. J. Gastroenterol. 112 (1), 18–35. https://doi.org/10.1038/ajg.2016.517.

Li, F., Wu, X., Zou, Y., Zhao, T., Zhang, M., Feng, W., Yang, L., 2012. Comparing antihyperglycemic activity and acute oral toxicity of three different trivalent chromium complexes in mice. Food Chem. Toxicol. 50 (5), 1623–1631. https://doi.org/10.1016/j.fct.2012.02.012.

Liu, Y., Sun, J., Rao, S., Su, Y., Li, J., Li, C., ... Yang, Y., 2013a. Antidiabetic activity of mycelia selenium-polysaccharide from Catathelasma ventricosum in STZ-induced diabetic mice. Food Chem. Toxicol. 62, 285–291. https://doi.org/10.1016/j.fct.2013.08.082.

Liu, Y., Sun, J., Rao, S., Su, Y., Yang, Y., 2013b. Antihyperglycemic, antihyperlipidemic and anti-oxidant activities of polysaccharides from Catathelasma ventricosum in streptozotocin-induced diabetic mice. Food Chem. Toxicol. 57, 39–45. https://doi.org/10.1016/j.fct.2013.03.001.

Michael, B., Yano, B., Sellers, R.S., Perry, R., Morton, D., Roome, N., ... Schafer, K., 2007. Evaluation of organ weights for rodent and non-rodent toxicity studies: a review of regulatory guidelines and a survey of current practices. Toxicol. Pathol. 35 (5), 742–750. https://doi.org/10.1080/01926230701595292.

Moron, M.S., Depierre, J.W., Mannervik, B., 1979. Levels of glutathione, glutathione reductase and glutathione S-transferase activities in rat lung and liver. Biochim. Biophys. Acta Gen. Subj. 582 (1), 67–78. https://doi.org/10.1016/0304-4165(79)90289-7.

Nabavi, S.F., Daglia, M., Moghaddam, A.H., Habtemariam, S., Nabavi, S.M., 2014. Curcumin and liver disease: from chemistry to medicine. Compr. Rev. Food Sci. Food Saf. 13 (1), 62–77. https://doi.org/10.1111/1541-4337.12047.

Nabavi, S.M., Nabavi, S.F., Eslami, S., Moghaddam, A.H., 2012. In vivo protective effects of quercetin against sodium fluoride-induced oxidative stress in the hepatic tissue. Food Chem. 132 (2), 931–935. https://doi.org/10.1016/j.foodchem.2011.11.070.

Nada, S.A., Omara, E.A., Abdel-Salam, O.M.E., Zahran, H.G., 2010. Mushroom insoluble polysaccharides prevent carbon tetrachloride-induced hepatotoxicity in rat. Food Chem. Toxicol. 48 (11), 3184–3188. https://doi.org/10.1016/j.fct.2010.08.019.

Neto, J.X.S., Pereira, M.L., Oliveira, J.T.A., Rocha-Bezerra, L.C.B., Lopes, T.D.P., Costa, H.P.S., ... Vasconcelos, I.M., 2017. A chitin-binding protein purified from moringa oleifera seeds presents anticandidal activity by increasing cell membrane permeability and reactive oxygen species production. Front. Microbiol. 8. https://doi.org/10.3389/fmicb.2017.00980.

Ohkawa, H., Ohishi, N., Yagi, K., 1979. Assay for lipid peroxides in animal tissues by thiobarbituric acid reaction. Anal. Biochem. 95 (2), 351–358. https://doi.org/10.1016/0003-2697(79)90738-3.

Peng, W., Yi-Meng, G., Xing, S., Na, G., Ji, L., Wei, W., ... Yu-Jie, F., 2017. Hepatoprotective effect of 2'-O-galloylhyperin against oxidative stress-induced liver damage through induction of Nrf2/ARE-mediated anti-oxidant pathway. Food Chem. Toxicol. 102, 129–142. https://doi.org/10.1016/j.fa2017.02.016.

Pinheiro Ferreira, P.M., Farias, D.F., de Abreu Oliveira, J.T., Urano Carvalho, A. d. F., 2008. Moringa oleifera: bioactive compounds and nutritional potential. Revista De Nutricao-Brazil. J. Nutrition 21 (4), 431–437. https://doi.org/10.1590/s1415-52732008000400007.

Qilong, W., Qiuxuan, Y., Xia, C., Qiuyu, W., Caleb, K.F., Min, G., ... Jiangnan, Y., 2018. Enhanced oral bioavailability and anti-gout activity of 6 -shogaol-loaded solid lipid nanoparticles. Int. J. Pharm. 550 (1–2), 24–34. https://doi.org/10.1016/j.ijpharm.2018.08.028.

Rajan, T.S., Giacoppo, S., Iori, R., De Nicola, G.R., Grassi, G., Pollastro, F., ... Mazzon, E., 2016. Anti-inflammatory and anti-oxidant effects of a combination of cannabidiol and moringin in LPS-stimulated macrophages. Fitoterapia 112, 104–115. https://doi.org/10.1016/j.fitote.2016.05.008.

Randriamboavonjy, J.I., Rio, M., Pacaud, P., Loirand, G., Tesse, A., 2017. Moringa oleifera seeds attenuate vascular oxidative and nitrosative stresses in spontaneously hypertensive rats. Oxidative Medicine and Cellular Longevity. https://doi.org/10.1155/2017/4129459.

Recknagel, R.O., Glende, E.A., Dolak, J.A., Waller, R.L., 1989. Mechanisms of carbon tetrachloride toxicity. Pharmacol. Ther. 43 (1), 139–154. https://doi.org/10.1016/0163-7258(89)90050-8.

Rotruck, J.T., Pope, A.L., Ganther, H.E., Swanson, A.B., Hafeman, D.G., Hoekstra, W.G., 1973. Selenium: biochemical role as a component of glutathione peroxidase. Science 179 (4073), 588–590. https://doi.org/10.1126/science.179.4073.588.

Sanches, S.C., Ramalho, L.N.Z., Mendes-Braz, M., Terra, V.A., Cecchini, R., Augusto, M.J., Ramalho, F.S., 2014. Riboflavin (vitamin B-2) reduces hepatocellular injury following liver ischaemia and reperfusion in mice. Food Chem. Toxicol. 67, 65–71.

https://doi.org/10.1016/j.fct.2014.02.013.
Shih-Yi, L., Ya-Yu, W., Wen-Ying, C., Su-Lan, L., Su-Tze, C., Ching-Ping, Y., Chun-Jung, C., 2017. Hepatoprotective activities of rosmarinic acid against extrahepatic cholestasis in rats. Food Chem. Toxicol. 108, 214–223. https://doi.org/10.1016/j.fct.2017.08.005.
Singh, R.S.G., Negi, P.S., Radha, C., 2013. Phenolic composition, anti-oxidant and anti-microbial activities of free and bound phenolic extracts of Moringa oleifera seed flour. J. Funct. Food. 5 (4), 1883–1891. https://doi.org/10.1016/j.jff.2013.09.009.
Sreelatha, S., Jeyachitra, A., Padma, P.R., 2011. Antiproliferation and induction of apoptosis by Moringa oleifera leaf extract on human cancer cells. Food Chem. Toxicol. 49 (6), 1270–1275. https://doi.org/10.1016/j.fct.2011.03.006.
Srinivasan, K., 2014. Anti-oxidant potential of spices and their active constituents. Crit. Rev. Food Sci. Nutr. 54 (3), 352–372. https://doi.org/10.1080/10408398.2011.585525.
Tong, S.S., Chu, C., Wei, Y.A., Wang, L., Gao, X.Z., Xu, X.M., Yu, J.N., 2011. Preparation and effects of 2,3-dehydrosilymarin, a promising and potent anti-oxidant and free radical scavenger. J. Pharm. Pharmacol. 63 (2), 238–244. https://doi.org/10.1111/j.2042-7158.2010.01210.x.
Torres, L.R.D., de Santana, F.C., Torres-Leal, F.L., de Melo, I.L.P., Yoshime, L.T., Matos-Neto, E.M., ... Mancini, J., 2016. Pequi (Caryocar brasiliense Camb.) almond oil attenuates carbon tetrachloride-induced acute hepatic injury in rats: anti-oxidant and anti-inflammatory effects. Food Chem. Toxicol. 97, 205–216. https://doi.org/10.1016/j.fct.2016.09.009.
Tsai, J.-C., Peng, W.-H., Chiu, T.-H., Huang, S.-C., Huang, T.-H., Lai, S.-C., ... Lee, C.-Y., 2010. Hepatoprotective effect of scoparia dulcis on carbon tetrachloride induced acute liver injury in mice. Am. J. Chin. Med. 38 (4), 761–775. https://doi.org/10.1142/s0192415x10008226.
Valko, M., Leibfritz, D., Moncol, J., Cronin, M.T.D., Mazur, M., Telser, J., 2007. Free radicals and anti-oxidants in normal physiological functions and human disease. Int. J. Biochem. Cell Biol. 39 (1), 44–84. https://doi.org/10.1016/j.biocel.2006.07.001.
Wang, Y., Gao, Y., Ding, H., Liu, S., Han, X., Gui, J., Liu, D., 2017. Subcritical ethanol extraction of flavonoids from Moringa oleifera leaf and evaluation of anti-oxidant activity. Food Chem. 218, 152–158. https://doi.org/10.1016/j.foodchem.2016.09.058.
Zhang, M.-h., Feng, L., Zhu, M.-m., Gu, J.-f., Jiang, J., Cheng, X.-d., ... Jia, X.-b., 2014. The anti-inflammation effect of Moutan Cortex on advanced glycation end products-induced rat mesangial cells dysfunction and High-glucose-fat diet and streptozotocin-induced diabetic nephropathy rats. J. Ethnopharmacol. 151 (1), 591–600. https://doi.org/10.1016/j.jep.2013.11.015.
Zhao, T., Fan, Y., Mao, G., Feng, W., Zou, Y., Zou, Y., ... Wu, X., 2017. Purification, characterization and anti-oxidant activities of enzymolysis polysaccharide from grifola frondosa. Iran. J. Pharm. Res. (IJPR) 16 (1), 347–356 Retrieved from < Go to ISI > ://WOS:000396490200031.
Zhou, Z., Tang, M., Liu, Y., Zhang, Z., Lu, R., Lu, J., 2017. Apigenin inhibits cell proliferation, migration, and invasion by targeting Akt in the A549 human lung cancer cell line. Anti Canccer Drugs 28 (4), 446–456. https://doi.org/10.1097/cad.0000000000000479.